

Optimization of Genomic Classifiers for Clinical Deployment: Evaluation of Bayesian Optimization to Select Predictive Models of Acute Infection and In-Hospital Mortality*

Michael B. Mayhew[†], Elizabeth Tran, Kirindi Choi, Uros Midic, Roland Luethy, Nandita Damaraju
and Ljubomir Buturovic

Inflammatix, Inc.

Burlingame, California 94010, USA

[†]*E-mail: mmayhew@inflammatix.com*

www.inflammatix.com

Acute infection, if not rapidly and accurately detected, can lead to sepsis, organ failure and even death. Current detection of acute infection as well as assessment of a patient's severity of illness are imperfect. Characterization of a patient's immune response by quantifying expression levels of specific genes from blood represents a potentially more timely and precise means of accomplishing both tasks. Machine learning methods provide a platform to leverage this *host response* for development of deployment-ready classification models. Prioritization of promising classifiers is dependent, in part, on hyperparameter optimization (HO) for which a number of approaches including grid search, random sampling and Bayesian optimization have been shown to be effective. We compare HO approaches for the development of diagnostic classifiers of acute infection and in-hospital mortality from gene expression of 29 diagnostic markers. We take a deployment-centered approach to our comprehensive analysis, accounting for heterogeneity in our multi-study patient cohort with our choices of dataset partitioning and hyperparameter optimization objective as well as assessing selected classifiers in external (as well as internal) validation. We find that classifiers selected by Bayesian optimization for in-hospital mortality can outperform those selected by grid search or random sampling. However, in contrast to previous research: 1) Bayesian optimization is not more efficient in selecting classifiers in all instances compared to grid search or random sampling-based methods and 2) we note marginal gains in classifier performance in only specific circumstances when using a common variant of Bayesian optimization (i.e. automatic relevance determination). Our analysis highlights the need for further practical, deployment-centered benchmarking of HO approaches in the healthcare context.

Keywords: hyperparameter optimization; Bayesian optimization; acute infection; sepsis; disease severity; mortality; classification; molecular diagnostics; genomics.

1. Introduction

Patient lives depend on the swiftness and accuracy of 1) assessment of the severity of their illness and 2) detection of acute infection (when present). The COVID-19 pandemic has put this fact into stark relief. Currently, clinicians determine severity of illness by computing scores

*Supplementary material can be found at <https://arxiv.org/abs/2003.12310>

(e.g. SOFA¹) based on patient physiological features associated with the risk of adverse events (e.g. in-hospital mortality, organ failure). Similarly, detection of acute infection generally involves evaluation of symptoms (e.g. cough, runny nose, fever) as well as laboratory tests for the presence of specific pathogens. However, these methods provide superficial and imprecise measures of patient illness. Recent work has highlighted the potential of using gene expression measurements from patient blood to detect the presence and type of infection to which the patient is responding²⁻⁵ as well as the patient’s severity of illness.⁶

Coupled with these host response signatures, advances in machine learning (ML) provide a platform for the development of robust, diagnostic classifiers of acute infection status (e.g. bacterial or viral) and in-hospital mortality from gene expression. An important step in this development is optimization of the classifier’s hyperparameters: aspects of the model that affect its complexity (e.g. penalty coefficient in a LASSO logistic regression) as well as how it’s trained (e.g. learning rates for stochastic gradient descent). Hyperparameter optimization begins with specification of a search space and proceeds by generating a user-specified number of hyperparameter configurations (HCs; sets of specific hyperparameter values corresponding to a unique classification model), training the classifier models given by each configuration, and evaluating the performance of the trained classifier in *internal validation*. Internal validation performance is typically assessed either on a separate validation/tuning dataset or by cross-validation. Hyperparameter configurations are then ranked by this performance, with the top configuration selected and retained for *external validation* (application to a held-out dataset).

Multiple HO approaches have been proposed. For classifiers with relatively small hyperparameter spaces (e.g. support vector machines), optimizing over a pre-defined grid of hyperparameter values (grid search; GS) has proven effective. More recent work has shown that optimization by randomly sampling (RS) hyperparameter configurations can lead to better coverage of high-dimensional hyperparameter spaces and potentially better classifier performance.⁷ Bayesian optimization (BO) is a global optimization procedure that has found success in applications as wide-ranging as viral capsid assembly,⁸ genetic pre-breeding,⁹ high-throughput RNA sequencing assembly¹⁰ and materials design.¹¹ BO has also proven effective for hyperparameter optimization in classical¹²⁻¹⁶ and biomedical¹⁷⁻²⁰ ML applications. In BO, one uses a model (commonly a Gaussian process (GP)²¹) to approximate the objective function one wants to optimize; for hyperparameter optimization, the objective function maps from hyperparameter configurations to the internal validation performance of their corresponding classifiers. In contrast to GS/RS, BO proceeds by sequentially evaluating configurations with each newly visited configuration used to update the model of the objective function.

In this work, we compare GS/RS and BO methods for hyperparameter optimization of gene expression-based diagnostic classifiers for two clinical tasks: 1) detection of acute infection and 2) prediction of mortality within 30 days of hospitalization. We optimize and train three different types of classifiers using gene expression features from 29 diagnostic markers in a multi-study cohort of 3413 patient samples for acute infection detection (3288 for 30-day mortality prediction). Patient samples were assayed on a variety of technical platforms and collected from a range of geographical regions, healthcare settings, and disease contexts. Our extensive analysis evaluates the BO approach, in particular, under a range of compu-

tational budgets and optimization settings. Crucially, beyond assessing and comparing the performance of top classifiers in internal validation, we further evaluate top models selected by all HO approaches in a multi-cohort external validation set comprising nearly 300 patients profiled by a targeted diagnostic instrument (NanoString). Our analysis provides important insights for diagnostic classifier development using genomic data, and, more generally, about the implementation and practical usage of HO methods in healthcare.

2. Related Work

Previous studies comparing HO approaches in the ML community have demonstrated that BO can select promising classifiers more efficiently (with fewer evaluations of hyperparameter configurations) than GS/RS methods.^{12–16,19,20,22} However, these studies have focused on internal validation performance and on benchmark datasets whose composition and handling (i.e. partitioning into training-validation-test splits) doesn't necessarily reflect characteristics of healthcare settings (i.e. smaller, structured, and more heterogeneous datasets; high propensity for models to be applied to out-of-distribution samples at test time).

Bayesian optimization has also found recent success in genomics and biomedical applications. Ghassemi et al.¹⁷ compare multiple HO approaches, including BO, for tuning parameters of the multi-scale entropy of heart rate time series to aid mortality prediction among sepsis patients. Colopy et al.¹⁸ analyzed RS and BO methods for optimization of patient-specific GP regression models used in vital-sign forecasting. A study by Nishio et al.¹⁹ evaluated both RBF SVM and XGBoost classifiers tuned by either RS or BO for detection of lung cancer from nodule CT scans. Borgli et al.²⁰ evaluated BO for tuning and transfer learning of pre-trained convolutional neural networks to detect gastrointestinal conditions from images. Again, however, these studies either reported internal validation performance or performance on a test set partitioned from a full (often small; on the order of 100s of samples) dataset that was collected from a single hospital, making conclusions difficult to draw about the generalizability of selected models in other segments of the deployment population. Moreover, these studies focused on: 1) no more than two classifier types, 2) a narrow range of settings for BO, and 3) physiological or image data. To our knowledge, no studies have evaluated the external validation performance of selected models, an important pre-requisite for eventual model deployment. In addition, no comparison of HO approaches has yet been attempted for development of diagnostic classifiers using genomic data.

3. Methods

3.1. Cohort & Feature Description

To build our datasets, we combined gene expression data from public sources and in-house clinical studies designed for research in diagnosing acute infections and sepsis. We collected the publicly available studies from the NCBI GEO and EMBL-EBI ArrayExpress databases using a systematic search.² The public studies were profiled using a variety of different technical platforms (e.g. mostly from microarrays). Samples from the in-house clinical studies were profiled on the NanoString nCounter platform using a custom codeset for 29 diagnostic genes of interest. All included studies consisted of samples from our target population, comprising

both adult and pediatric patients from diverse geographical regions and clinical settings. Each included study had measurements taken from patient blood for all 29 markers.

The features we used in our analyses were based on the expression values of 29 genes previously found to accurately discriminate three different aspects of acute infection: 1) viral vs. bacterial infection (7 genes),³ 2) infection vs. non-infectious inflammation (11 genes),² and 3) high vs. low risk of 30-day mortality (11 genes).⁶ Building on our previous work,⁵ we computed both the geometric means and arithmetic means of these six groups of genes, producing 12 features. We optimized and trained our classifiers on the combination of these 12 features and the expression values of all 29 genes (41 features in total). Labels for one of three classes of the acute infection detection or BVN task (**B**acterial infection, **V**iral infection, or **N**on-infectious inflammation) were determined by multiple-physician adjudication after chart review and not necessarily by positive pathogen identification. Non-infected determinations did not include healthy controls. Binary indicator labels of whether a patient died within 30 days of hospitalization were used for the mortality task. We derived these labels from study metadata (when available) and the associated study’s manuscripts.

For both tasks, we separated studies into a training set and an external validation set. For the BVN task, the training set consisted of 43 studies (profiled outside Inflammatrix) and 3413 patients (1087 with bacterial infection, 1244 with viral infection, and 1082 non-infected). The BVN external validation set consisted of six studies (profiled by Inflammatrix) and 293 patients (153 with bacterial infection, 106 with viral infection, and 34 non-infected). For the mortality task, the training set consisted of 33 studies (profiled outside Inflammatrix) and 3288 patients (175 30-day mortality events) while the mortality external validation set comprised four studies (profiled by Inflammatrix) and 348 patients (80 30-day mortality events).

3.2. Grouped cross-validation

Previous analyses by our group⁵ suggested that alternative cross-validation strategies were preferable over conventional k-fold CV for identifying classifiers able to generalize across heterogeneous patient populations. We use 5-fold grouped CV (full studies are allocated to one and only one of five folds) to rank and select hyperparameter configurations from GS/RS methods and as an objective function in BO.

3.3. Classifier types and performance assessment

We evaluated three types of classification models: 1) support vector machines with a radial basis function (RBF) kernel, 2) XGBoost (XGB²³) and 3) multi-layer perceptrons (MLP). MLP models were trained with the Adam optimizer²⁴ with mini-batch size fixed at 128.

For the BVN task, we ranked and selected models based on multi-class AUC (mAUC).²⁵ For the mortality task, we used binary AUC as our performance metric. We opted for AUC (as opposed to other metrics suited to class imbalance in the mortality task) due to its clinical acceptance. To determine performance of models in grouped 5-fold CV, we pooled the model’s predicted probabilities for each fold and computed the relevant metric (mAUC or AUC) from the pooled probabilities. The top hyperparameter configuration for each task and optimization run was then trained on the full training set and applied to the external validation set.

We computed external validation performance (either mAUC or AUC) for these top models using their predicted probabilities for the validation samples. We computed 95% bootstrap confidence intervals for differences in classification performance by sampling predicted probabilities with replacement 5000 times (using the same set of bootstrap sample IDs for both sets of predicted probabilities in the comparison), computing the relevant performance metric on each bootstrap sample, computing the difference between performance metrics for each bootstrap sample in a given comparison, and reporting the 2.5th and 97.5th quantiles of the 5000 bootstrap samples of the differences.

3.4. *Hyperparameter optimization details*

For RBF SVM, we conduct a grid search over configurations of the cost, C , and bandwidth hyperparameters, γ . C values ranged from 1e-03 to 2.15 and γ values ranged from 1.12e-04 to 10. We generated RS samples for XGBoost and MLP uniformly and independently of one another from pre-specified ranges or from grids (Suppl. Tables 1 and 2).

In our analyses with BO, the objective function maps from hyperparameter configurations to 5-fold grouped CV performance of the corresponding classifiers. The two main components of BO are: 1) a model that approximates the objective function, and 2) an acquisition function to propose the next configuration to visit in hyperparameter space. We use a GP regression model with Gaussian noise to approximate the objective function. Each BO run consists of two stages: 1) initialization and 2) optimization. In the initialization stage, we uniformly and independently sample configurations (either 5 or 25) from the hyperparameter space to seed construction of the GP approximation of the objective function.

We investigate both the expected improvement (EI) and upper confidence bound (UCB) acquisition functions. We use both standard and automatic relevance determination (ARD) forms of the Matern5/2 covariance function in BO’s GP model of the objective (further details in Supplement). We also perform BO in the hyperparameters’ native scales (*original space*) or in which continuous and discrete hyperparameter dimensions are searched in the continuous range 0 to 1 and transformed back to their native scales prior to their evaluation (*transformed*).

4. Results

We compared BO and GS/RS approaches for hyperparameter optimization of three types of classifiers for two clinical tasks. For the BVN task, we sought classifiers that could achieve high performance in predicting whether a patient had a bacterial or viral infection or was showing a non-infectious inflammatory response. For the mortality task, we sought classifiers that could achieve high performance in predicting mortality events within 30 days of hospital admission. Though we considered BO at two initialization budgets (5 and 25 configurations), we did not see substantial differences in performance between classifiers with 5 and 25 initial configurations (Suppl. Table 3, Suppl. Figs. 1 and 2). We focus on BO results with 25 initial configurations and the EI acquisition function for the remainder of this work.

General comparison of classifier performance across tasks and HO approaches

Across both tasks and HO approaches, we note distinct performance characteristics of the selected classifiers of each type. While RBF SVM classifiers performed similarly to the other

two classifier types on the BVN task, they were the worst performers on the mortality task. XGB classifiers selected by either RS or BO demonstrated competitive performance in both tasks and were remarkably consistent in their performance regardless of the number of hyperparameter configurations evaluated for HO. MLPs achieved the highest internal and external validation performance for both acute infection detection and mortality prediction (Table 1), suggesting potential benefits of learning latent features (hidden layers) for these tasks.

Model	HO Type	No. of Evals.	ARD	BVN CV	BVN Val.	Mort. CV	Mort. Val.
RBF	GS	10	-	0.808	0.862	0.758	0.736
	GS	50	-	0.814	0.853	0.797	0.739
	GS	100	-	0.814	0.853	0.800	0.782
	GS	250	-	0.814	0.853	0.801	0.749
	GS	500	-	0.815	0.853	0.801	0.749
	GS	1000	-	0.815	0.853	0.839	0.708
	GS	5000*	-	0.815	0.853	0.839	0.708
	BO	10	Y	0.811	0.788	0.800	0.747
	BO	10	N	0.815	0.851	0.800	0.746
	BO	50	Y	0.816	0.852	0.801	0.752
	BO	50	N	0.816	0.852	0.801	0.749
	BO	100	Y	0.816	0.852	0.800	0.753
BO	100	N	0.816	0.852	0.801	0.752	
XGB	RS	50	-	0.809	0.830	0.880	0.819
	RS	100	-	0.813	0.827	0.885	0.819
	RS	250	-	0.812	0.826	0.885	0.829
	RS	500	-	0.810	0.829	0.885	0.826
	RS	1000	-	0.810	0.822	0.885	0.822
	RS	5000	-	0.813	0.830	0.888	0.823
	RS	25000	-	0.815	0.860	0.889	0.816
	BO	50	Y	0.818	0.865	0.887	0.814
	BO	50	N	0.812	0.828	0.881	0.817
	BO	100	Y	0.811	0.825	0.885	0.825
	BO	100	N	0.809	0.826	0.878	0.817
	BO	250	Y	0.818	0.865	0.886	0.826
	BO	250	N	0.816	0.834	0.882	0.802
	BO	500	Y	0.818	0.865	0.889	0.827
	BO	500	N	0.812	0.831	0.880	0.815
	MLP	RS	50	-	0.818	0.860	0.763
RS		100	-	0.814	0.863	0.785	0.640
RS		250	-	0.824	0.861	0.807	0.625
RS		500	-	0.819	0.859	0.853	0.691
RS		1000	-	0.835	0.872	0.809	0.637
RS		5000	-	0.837	0.835	0.826	0.796
RS		25000	-	0.840	0.856	0.859	0.743
BO		50	Y	0.816	0.820	0.888	0.823
BO		50	N	0.814	0.824	0.888	0.820
BO		100	Y	0.822	0.845	0.886	0.847
BO		100	N	0.828	0.854	0.884	0.825
BO		250	Y	0.817	0.848	0.890	0.842
BO		250	N	0.832	0.832	0.889	0.812
BO		500	Y	0.837	0.855	0.894	0.835
BO		500	N	0.826	0.822	0.890	0.806

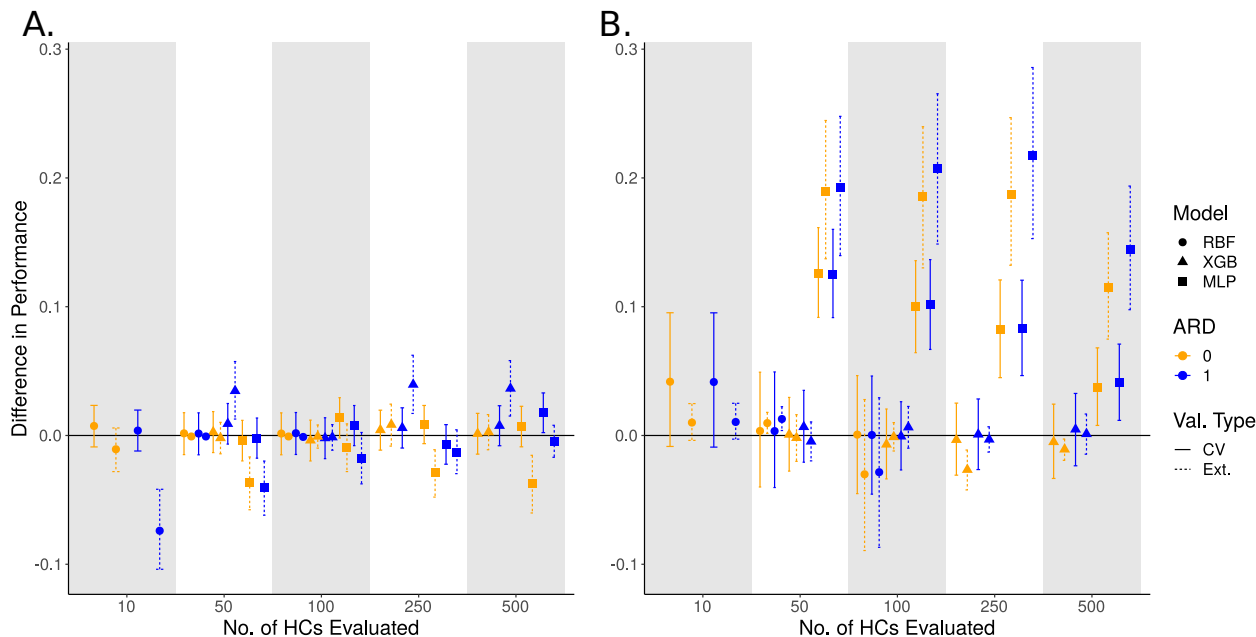


Fig. 1. Differences in classification performance (points) on the BVN (A; mAUC) and mortality (B; AUC) tasks for BO evaluation budgets. Differences greater than 0 indicate better performance for the BO-selected classifier. Classifiers were selected using either BO or GS/RS with the indicated number of HCs evaluated. Error bars represent 95% bootstrap confidence intervals of the difference in performance.

Evaluation of BO- and GS/RS-selected classifiers at evaluation budgets typical of BO. Previous studies have shown that BO can select promising classifiers more efficiently (with fewer evaluations of hyperparameter configurations) than GS/RS methods. Surprisingly, we find that at smaller numbers of configurations evaluated (more typical of BO), classifiers selected by GS/RS showed similar or better performance in both internal and external validation (Table 1 and Figs. 1) when compared with corresponding BO-selected classifiers. We observed similar trends when using the UCB acquisition function (Suppl. Fig. 3 and Suppl. Table 4) or the transformed hyperparameter space (Suppl. Fig. 5 and Suppl. Table 5). However, we do note two specific instances in which BO-selected classifiers exceeded performance of GS/RS-selected classifiers at smaller numbers of evaluated configurations: 1) XGBoost classifiers in external validation for the BVN task and 2) MLP classifiers for the mortality task. While these two instances are consistent with prior findings of BO’s relative efficiency in selecting classifiers, our results also suggest that simply committing to one HO approach over another could miss models that generalize well and that performance of top selected classifiers depends on the task and classifier type as well as the approach to HO.

Evaluation of BO- and GS/RS-selected classifiers at evaluation budgets typical of GS/RS. In the previous analysis, we compared BO- and GS/RS-selected classifiers at evaluation budgets typical of BO (i.e. fewer configurations evaluated). In Figure 2, we compare BO-selected classifiers from their highest evaluation budgets (100 evaluations for RBF and 500

evaluations for XGB and MLP) to classifiers selected by GS/RS at larger evaluation budgets. Interestingly, we find that the BO-selected MLP classifiers for the mortality task continue to outperform their corresponding RS-selected counterparts, even with 25000 configurations evaluated for RS. Similarly, we find that BO-selected XGBoost classifiers exceed external validation performance of RS-selected classifiers on the BVN task up to an RS evaluation budget of 25000 configurations (though the differences do not persist at 25000 configurations). We observe these performance differences when conducting BO with the UCB (vs. EI) acquisition function or with a transformed hyperparameter space (Suppl. Figs. 4 and 6). These results indicate the relative efficiency of BO in candidate classifier selection in these two instances but also illustrate the competitiveness of GS/RS-selected classifiers in our setting.

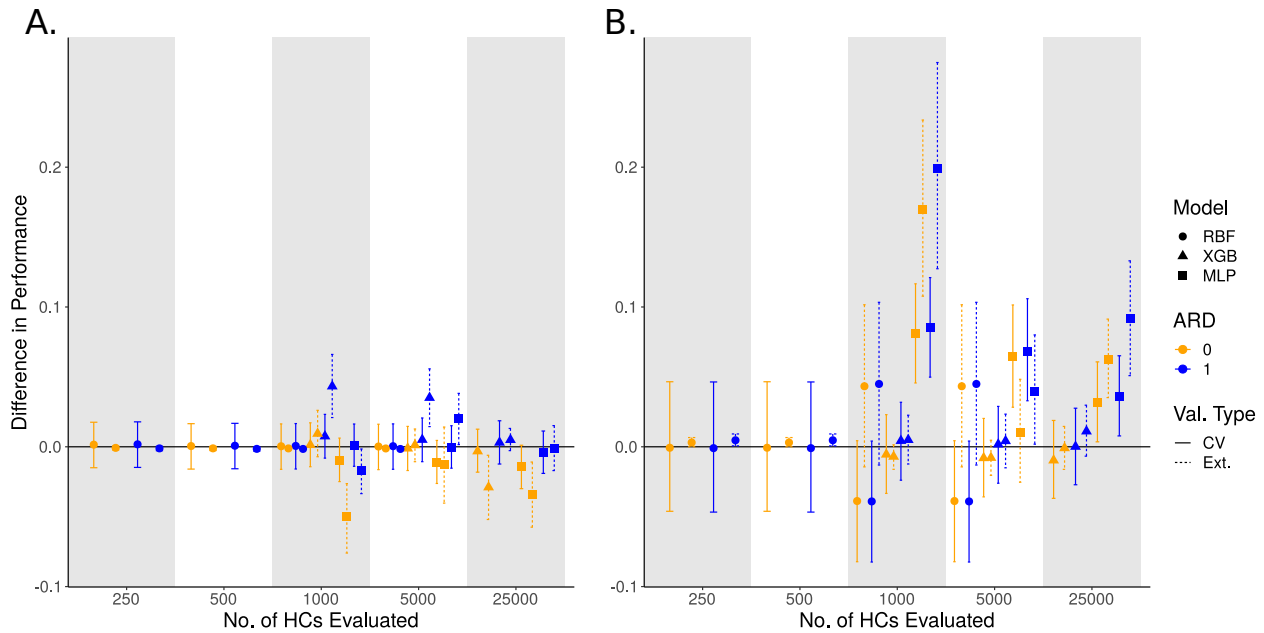


Fig. 2. Differences in classification performance on the BVN (A; mAUC) and mortality (B; AUC) tasks for GS/RS evaluation budgets. Here, indicated evaluation budgets apply to GS/RS-selected classifiers, whereas BO-selected classifiers are taken from 100-evaluation (RBF) or 500-evaluation (XGB and MLP) runs.

Assessment of effects on classifier performance of automatic relevance determination in BO. For high-dimensional hyperparameter spaces, some hyperparameters may have a greater impact on the model’s generalization performance than others. Automatic relevance determination (ARD²⁶) in the GP model of BO’s objective provides the means to estimate effects of variations in hyperparameter dimensions on the objective’s value and has been used in multiple implementations of BO (e.g. Snoek et al., 2012¹² and BoTorch, <https://botorch.org/docs/models>). We directly compare the internal and external validation performance of classifiers selected by BO with and without ARD. In Figure 3, we find that enabling ARD seems to lead to comparable if not slightly better internal validation performance at higher evaluation budgets. Moreover, enabling ARD seems to improve exter-

nal validation performance for both XGB (BVN task) and MLP classifiers (both tasks). In fact, the highest external validation performance by XGB classifiers on the BVN task is only achieved with ARD enabled (Table 1). However, these differences in classifier performance are not as evident when using the UCB acquisition function (Suppl. Fig. 7) or conducting BO with a transformed version of the hyperparameter space (Suppl. Fig. 8). Thus, ARD may not be necessary to select top-performing diagnostic classifiers for these two clinical tasks.

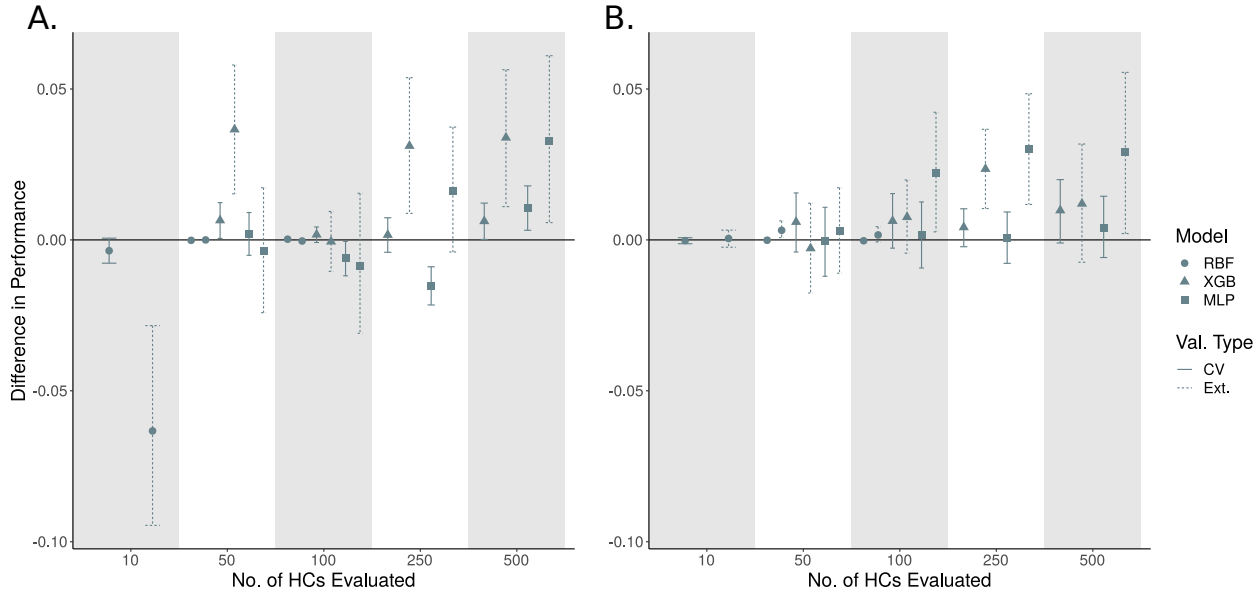


Fig. 3. Differences in classification performance on the BVN (A; mAUC) and mortality (B; AUC) tasks for BO-selected classifiers with or without ARD enabled (EI acquisition function, 25 initialization configurations). Differences greater than 0 indicate better performance for the ARD-enabled classifier. Error bars represent 95% bootstrap confidence intervals of the difference in performance.

5. Discussion & Conclusions

In this analysis, we carried out a comprehensive comparison of HO approaches for diagnostic classifier development to determine what approach (if any) led to improvements in: 1) external validation performance or 2) computational efficiency. Consistent with previous findings, we found that BO was able to prioritize candidate classifiers for two tasks relevant to emergency and critical care with a fraction of the configurations evaluated using GS/RS. As embarrassingly parallel approaches like GS/RS can necessitate the use of commodity computing clusters, BO’s efficiency makes the approach a potentially cost-effective alternative to HO. We also found that the external validation performance of MLP classifiers selected by BO for prediction of in-hospital mortality was consistently better across a range of HO evaluation budgets than the performance of classifiers selected by GS/RS, highlighting BO’s potential to uncover diagnostic classifiers that generalize better to unseen patients.

However, and in contrast to previous comparisons of HO approaches, our analyses indicated that GS/RS methods could select classifiers for both tasks with evaluation budgets comparable to those used for BO. We also found mixed evidence in support of enabling ARD in the kernel

of BO’s GP model of the objective function. Thus, while we hoped we would uncover distinct and general differences between HO approaches in order to develop better guidelines about when (or even if) to use one approach over another, we did not identify such clear differences across tasks, classifier types, and optimization settings. Rather, our analysis suggests that both GS/RS and BO approaches should be investigated for classifier development.

We acknowledge limitations of our approach. For our RS runs, we sampled configurations uniformly and independently from pre-defined ranges or grids of values. Other random sampling approaches could’ve been used in which configurations are generated dependent on the values of previously generated configurations (e.g. Latin hypercube or low-discrepancy Sobol sequences) in order to encourage diversity of the resulting sample.⁷ A second limitation is that we used a single set of features derived from a previously identified set of 29 gene expression markers. We chose these features based on previous analyses⁵ and consistent with our goal of developing diagnostic classifiers from these specific markers for clinical deployment. We acknowledge our conclusions may not hold with other feature sets.

Throughout this work, we were mindful of the larger implications of HO on downstream clinical deployment. Our choice of objective function (grouped 5-fold CV performance) and our evaluation of performance in external validation were based on our experiences with the smaller, more heterogeneous data regimes typical of biomedical research as well as our expectation that we had likely not fully characterized the deployment population (patients to which we would apply our selected classifiers). In our survey of other comparative studies of HO, we noted important connections between assumptions about the deployment scenario and about how well the deployment population was characterized by the training data with study design choices about dataset partitioning and the objective function. For example, ML studies primarily focused on larger ($N > \sim 100k$) datasets composed mainly of natural images. These benchmarks were often constructed (e.g. MNIST; <http://yann.lecun.com/exdb/mnist/>) to satisfy the assumption that the distribution of training and external validation samples are similar if not the same. In this setting, one would expect that the correspondence between a model’s internal and external validation performance should be strong: a model with the best performance in optimization should have nearly the best, if not the best, performance in a held-out dataset. Thus, optimizing a classifier in internal validation would be advisable, especially when the training dataset fully captures the characteristics of the target population.

However, patient data is known to be heterogeneous due to biological differences as well as differences in geography, healthcare delivery, and assay technologies used, suggesting that the assumption of distributional similarity between training and external validation samples is likely to be violated. A recent study by Google highlighted this challenge for deployment in healthcare: their AI system for breast cancer screening showed drops in predictive performance when trained on mammograms from the UK and applied to mammograms from the US.²⁷ Our recent work also found that estimates of generalization performance from internal validation can be optimistically biased, even when accounting for technical/biological heterogeneity.⁵

Thus, regardless of the HO approach used, simply optimizing for internal validation performance may still lead to overfitting of the resulting classifier. Thus, care should be taken before rote application of HO techniques to ensure that the dataset partitioning, choice of objective

function, and, if possible, use of external validation data best account for characteristics of the target population and the deployment scenario. For example, if deploying in a single hospital or in a well-characterized or homogeneous population, performance of a candidate classifier in conventional k-fold CV or on a held-out validation set may suffice for optimization and one might expect good correspondence between internal and external validation performance. In our setting, however, we assume that we have not fully characterized our target population, owing to considerable patient heterogeneity and our desired deployment in multiple health-care settings worldwide. Consequently, we opt for grouped k-fold CV as our internal validation method and use our external validation performance to aid model selection.

In conclusion, we find that both GS/RS and BO remain promising avenues for hyperparameter optimization and represent key components in the development of more effective diagnostics for emergency and critical care.

References

1. A. E. Jones, S. Trzeciak and J. A. Kline, The Sequential Organ Failure Assessment score for predicting outcome in patients with severe sepsis and evidence of hypoperfusion at the time of emergency department presentation, *Critical care medicine* **37**, 1649 (May 2009), 19325482[pmid].
2. T. Sweeney, A. Shidham, H. R. Wong and P. Khatri, A comprehensive time-course-based multicohort analysis of sepsis and sterile inflammation reveals a robust diagnostic gene set, *Science Translational Medicine* **7** (2015).
3. T. Sweeney, H. R. Wong and P. Khatri, Robust classification of bacterial and viral infections via integrated host gene expression diagnostics, *Science Translational Medicine* **8** (2016).
4. T. Sweeney and P. Khatri, Benchmarking sepsis gene expression diagnostics using public data, *Critical care medicine* **45**, p. 1 (2017).
5. M. B. Mayhew, L. Buturovic, R. Luethy, U. Midic, A. R. Moore, J. A. Roque, B. D. Shaller, T. Asuni, D. Rawling, M. Rimmel, K. Choi, J. Wacker, P. Khatri, A. J. Rogers and T. E. Sweeney, A generalizable 29-mrna neural-network classifier for acute bacterial and viral infections, *Nature Communications* **11**, p. 1177 (2020).
6. T. Sweeney, T. Perumal and R. e. a. Henao, A community approach to mortality prediction in sepsis via gene expression analysis, *Nat Commun* (2018).
7. J. Bergstra and Y. Bengio, Random search for hyper-parameter optimization, *Journal of Machine Learning Research* **13**, 281 (2012).
8. M. Thomas and R. Schwartz, A method for efficient Bayesian optimization of self-assembly systems from scattering data, *BMC Systems Biology* **12**, p. 65 (2018).
9. R. Tanaka and H. Iwata, Bayesian optimization for genomic selection: a method for discovering the best genotype among a large number of candidates., *Theor Appl Genet* **131**, 93 (2018).
10. S. Mao, Y. Jiang, E. B. Mathew and S. Kannan, BOAssembler: a Bayesian Optimization Framework to Improve RNA-Seq Assembly Performance (2019).
11. Y. Zhang, D. W. Apley and W. Chen, Bayesian Optimization for Materials Design with Mixed Quantitative and Qualitative Variables, *Scientific Reports* **10**, p. 4924 (2020).
12. J. Snoek, H. Larochelle and R. P. Adams, Practical Bayesian optimization of machine learning algorithms, *In Advances in neural information processing systems* , 2951 (2012).
13. J. Snoek, O. Rippel, K. Swersky, R. Kiros, N. Satish, N. Sundaram, M. Patwary, M. Prabhat and R. Adams, Scalable Bayesian optimization using deep neural networks, in *International conference on machine learning*, 2015.
14. A. Klein, S. Falkner, S. Bartels, P. Hennig and F. Hutter, Fast Bayesian Optimization of Machine Learning Hyperparameters on Large Datasets, in *Proceedings of the 20th International Confer-*

- ence on Artificial Intelligence and Statistics*, eds. A. Singh and J. Zhu, Proceedings of Machine Learning Research, Vol. 54 (PMLR, Fort Lauderdale, FL, USA, 20–22 Apr 2017).
15. S. Falkner, A. Klein and F. Hutter, BOHB: Fast and Efficient Hyperparameter Optimization at Scale, in *ICML*, 2018.
 16. A. Klein, Z. Dai, F. Hutter, N. Lawrence and J. Gonzalez, Meta-Surrogate Benchmarking for Hyperparameter Optimization, in *Advances in Neural Information Processing Systems 32*, eds. H. Wallach, H. Larochelle, A. Beygelzimer, F. d’Alché Buc, E. Fox and R. Garnett (Curran Associates, Inc., 2019) pp. 6270–6280.
 17. M. Ghassemi, L. Lehman, J. Snoek and S. Nemati, Global optimization approaches for parameter tuning in biomedical signal processing: A focus on multi-scale entropy, in *Computing in Cardiology 2014*, Sep. 2014.
 18. G. W. Colopy, S. J. Roberts and D. A. Clifton, Bayesian Optimization of Personalized Models for Patient Vital-Sign Monitoring, *IEEE Journal of Biomedical and Health Informatics* **22**, 301 (March 2018).
 19. M. Nishio, M. Nishizawa, O. Sugiyama, R. Kojima, M. Yakami, T. Kuroda and K. Togashi, Computer-aided diagnosis of lung nodule using gradient tree boosting and Bayesian optimization, *PloS one* **13**, e0195875 (Apr 2018), 29672639[pmid].
 20. R. J. Borgli, H. Kvale Stensland, M. A. Riegler and P. Halvorsen, Automatic Hyperparameter Optimization for Transfer Learning on Medical Image Datasets Using Bayesian Optimization, in *2019 13th International Symposium on Medical Information and Communication Technology (ISMICT)*, May 2019.
 21. C. E. Rasmussen and C. K. I. Williams, *Gaussian Processes for Machine Learning* (The MIT Press, 2006).
 22. J. Bergstra, D. Yamins and D. D. Cox, Making a science of model search: Hyperparameter optimization in hundreds of dimensions for vision architectures (2013).
 23. T. Chen and C. Guestrin, XGBoost: A Scalable Tree Boosting System, in *Proceedings of the 22nd ACM SIGKDD International Conference on Knowledge Discovery and Data Mining*, KDD ’16 (ACM, New York, NY, USA, 2016).
 24. D. P. Kingma and J. Ba, Adam: A Method for Stochastic Optimization (2014).
 25. D. J. Hand and R. J. Till, A simple generalisation of the area under the ROC curve for multiple class classification problems, *Machine learning* **45**, 171 (2001).
 26. R. M. Neal, *Bayesian Learning for Neural Networks* (Springer-Verlag, Berlin, Heidelberg, 1996).
 27. S. M. McKinney, M. Sieniek, V. Godbole, J. Godwin, N. Antropova, H. Ashrafiyan, T. Back, M. Chesus, G. C. Corrado, A. Darzi, M. Etemadi, F. Garcia-Vicente, F. J. Gilbert, M. Halling-Brown, D. Hassabis, S. Jansen, A. Karthikesalingam, C. J. Kelly, D. King, J. R. Ledsam, D. Melnick, H. Mostofi, L. Peng, J. J. Reicher, B. Romera-Paredes, R. Sidebottom, M. Suleyman, D. Tse, K. C. Young, J. De Fauw and S. Shetty, International evaluation of an AI system for breast cancer screening, *Nature* **577**, 89 (2020).

Supplementary Material for “Optimization of Genomic Classifiers for Clinical Deployment: Evaluation of Bayesian Optimization to Select Predictive Models of Acute Infection and In-Hospital Mortality”

Michael B. Mayhew¹, Elizabeth Tran¹, Kirindi Choi¹, Uros Midic¹, Roland Luethy¹, Nandita Damaraju¹, and Ljubomir Buturovic¹

¹Inflammatix, Inc., Burlingame, CA USA 94010

Gene expression features & data processing

The features we used in our analyses were based on the expression values of 29 genes previously found to accurately discriminate three different aspects of acute infection: 1) viral vs. bacterial infection (7 genes) [4], 2) infection vs. non-infectious inflammation (11 genes) [3], and 3) high vs. low risk of 30-day mortality (11 genes) [2]. The 29 genes were grouped into six modules based on positive or negative correlation with infection status or mortality risk: increased expression in viral infections (IFI27, JUP, LAX1), increased expression in bacterial infections (TNIP1, CTSS, HK3, GPAA1), increased (HIF1A, SEPP1, RGS1, C11orf74, CD163, PER1, DEFA4, CIT) and decreased (LY86, TST, KCNJ2) expression in patients who died within 28 days of hospitalization, increased (CEACAM1, ZDHHC19, C9orf95, GNA15, BATF, C3AR1) and decreased (KIAA1370, TGFBI, MTCH1, RPGRIP1, HLA-DPB1) expression in patients with sepsis. Building on our previous work [1], we computed both the geometric means and arithmetic means of these six groups of genes, producing 12 features. We optimized and trained our classifiers on the combination of these 12 features and the expression values of all 29 genes (41 features in total).

We extracted gene expression measurements for all 29 diagnostic markers of interest and normalized these raw expression values for each study. To account for technical and biological heterogeneity across the expression studies, we then performed co-normalization (see [1]). We also collected labels for patient infection and mortality status. Labels for one of three classes of the BVN task were determined by multiple-physician adjudication after chart review and not necessarily by positive pathogen identification. Non-infected determinations did not include healthy controls. Binary indicator labels of whether a patient died within 30 days of hospitalization were used for the mortality task. We derived these labels from study metadata (when available) and the associated study’s manuscripts.

Bayesian optimization details

We evaluate Bayesian optimization with two different initialization budgets: 5 and 25 initial configurations. Our BO analyses considered both the expected improvement (EI) and upper confidence bound (UCB) acquisition functions. We used the Matern5/2 kernel in BO’s GP model of the objective function:

$$k(r) = \sigma^2 \left(1 + \sqrt{5}r + \frac{5}{3}r^2 \right) \exp(-\sqrt{5}r) \quad (1)$$

where

$$r = \sqrt{\sum_{h=1}^H \frac{(x_h - x'_h)^2}{\sigma_l^2}}. \quad (2)$$

Here H is the dimensionality of the hyperparameter space, x and x' are two configuration vectors being compared, σ^2 is the variance in the objective function’s value and σ_l is a lengthscale parameter that modulates the effect of changes in the hyperparameter dimensions on changes in grouped 5-fold CV performance. In this formulation, there is a single lengthscale parameter for all hyperparameter dimensions. We also assess the automatic relevance determination (ARD) form of the Matern5/2 kernel in which each hyperparameter dimension has their own lengthscale parameter:

$$r = \sqrt{\sum_{h=1}^H \frac{(x_h - x'_h)^2}{\sigma_{l,h}^2}} \quad (3)$$

Implementation details

We used the RBF SVM implementation in Python3’s `scikit-learn` module (version 0.20.1). For XGBoost analyses, we used the `scikit-learn` API in the `xgboost` package (version 0.90). All MLP models were implemented using `Keras` (version 2.1.6) with a `TensorFlow` (version 1.8.0) back-end. We carried out all GS/RS analyses using our proprietary distributed HO software. In our parallelized implementation of GS/RS, we first generate all configurations and then distribute the configurations to multiple compute nodes in a commodity cluster for evaluation. We executed each GS/RS run using 100 `t3a.large` instances (2 vCPUs/instance) from Amazon Web Services (AWS). We implemented BO analyses with the `GPyOpt` package [5] and carried out BO on a personal laptop with an Intel Core i7-8550U at 1.80GHz 8-core CPU, running Ubuntu 18.04.

Hyperparameter space details

Table 1: XGBoost hyperparameter space. Shown are the values (for discrete and categorical hyperparameters) and ranges (for continuous hyperparameters) over which optimization runs were conducted. We refer interested readers to <https://xgboost.readthedocs.io/en/latest/parameter.html> for a more in-depth description of the different hyperparameters. Where relevant, we indicate when continuous hyperparameters were optimized in log scale and subsequently transformed. All other model parameters were left at default values.

Hyperparameter	Type	Values
booster	categorical	['gbtree', 'gblinear', 'dart']
gamma	continuous	(0,5)
learning rate (eta)	continuous	(0.001,0.1)
L1 regularization term (alpha)	continuous	(0,1)
L2 regularization term (lambda)	continuous	(0,4.5)
maximum delta step	discrete	[0,1]
maximum tree depth	discrete	[3,4,5,6,7,8,9,10]
minimum child weight	discrete	[1,2,3,4,5]
number of boosting rounds	continuous (log)	(4.60517,6.907755)
subsample ratio of columns for each level	continuous	(0.7,1)
subsample ratio of columns for each node	continuous	(0.5,1)
subsample ratio of columns for each tree	continuous	(0.7,1)
subsample ratio of training instances	continuous	(0.3,1)

Table 2: MLP hyperparameter space. Shown are the values (for discrete and categorical hyperparameters) and ranges (for continuous hyperparameters) over which optimization runs were conducted. Where relevant, we indicate when continuous hyperparameters were optimized in log scale and subsequently transformed or optimized on a continuous range and converted to the nearest integer (int).

Hyperparameter	Type	Values
training iterations	discrete	[50,100,250,500,1000,2500]
number of hidden layers	discrete	[1,2,3,4,5]
number of nodes per hidden layer	discrete	[2,3,4,5,6,7,8,9,10,11,12,13,14,15,16,17,18,19,20,21]
activation type	categorical	['ELU', 'ReLU', 'sigmoid', 'tanh', 'Leaky ReLU']
perform dropout?	categorical	[True,False]
dropout rate (input layer)	continuous	(0.0,0.5)
dropout rate (fully-connected layers)	continuous	(0.0,0.5)
weight regularization type	categorical	['None', 'L1', 'L2']
L1 regularization term	continuous (log)	(-11.512925464970229,0.0)
L2 regularization term	continuous (log)	(-11.512925464970229, 0.0)
learning rate	continuous (log)	(-11.512925464970229, -2.3025850929940455)
weight initialization seed	discrete	[10,11,12,....,10000]

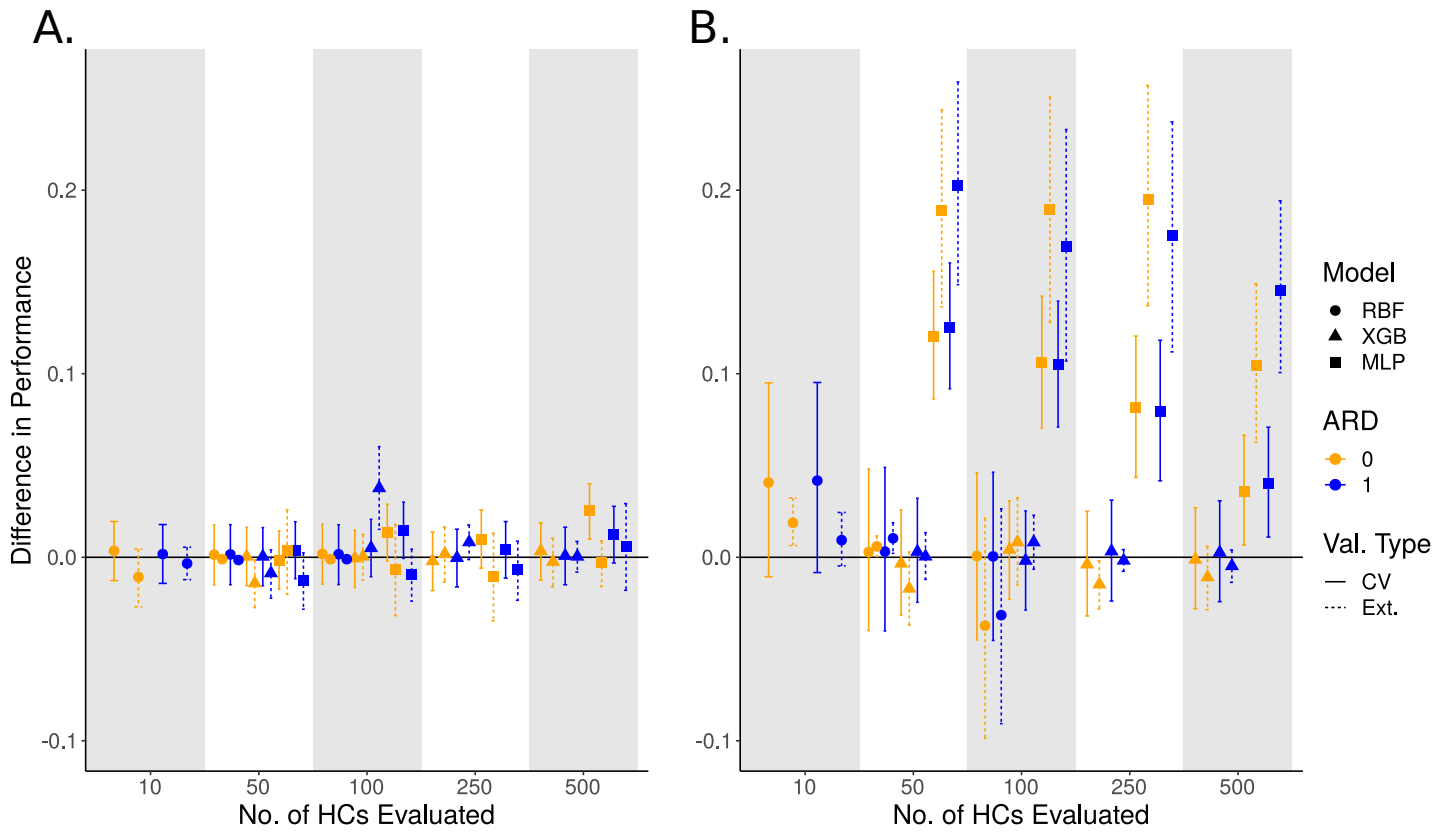


Figure 1: Differences in classifier performance in internal (CV) and external validation on the BVN (A; mAUC) and mortality (B; AUC) tasks for BO evaluation budgets with the EI acquisition function and 5 initialization configurations in the *original* hyperparameter space. Differences greater than 0 indicate better performance for the BO-selected classifier. Classifiers were selected using either BO or GS/RS with the indicated number of evaluations. Points represent observed differences while error bars represent 95% bootstrap confidence intervals of the difference in performance.

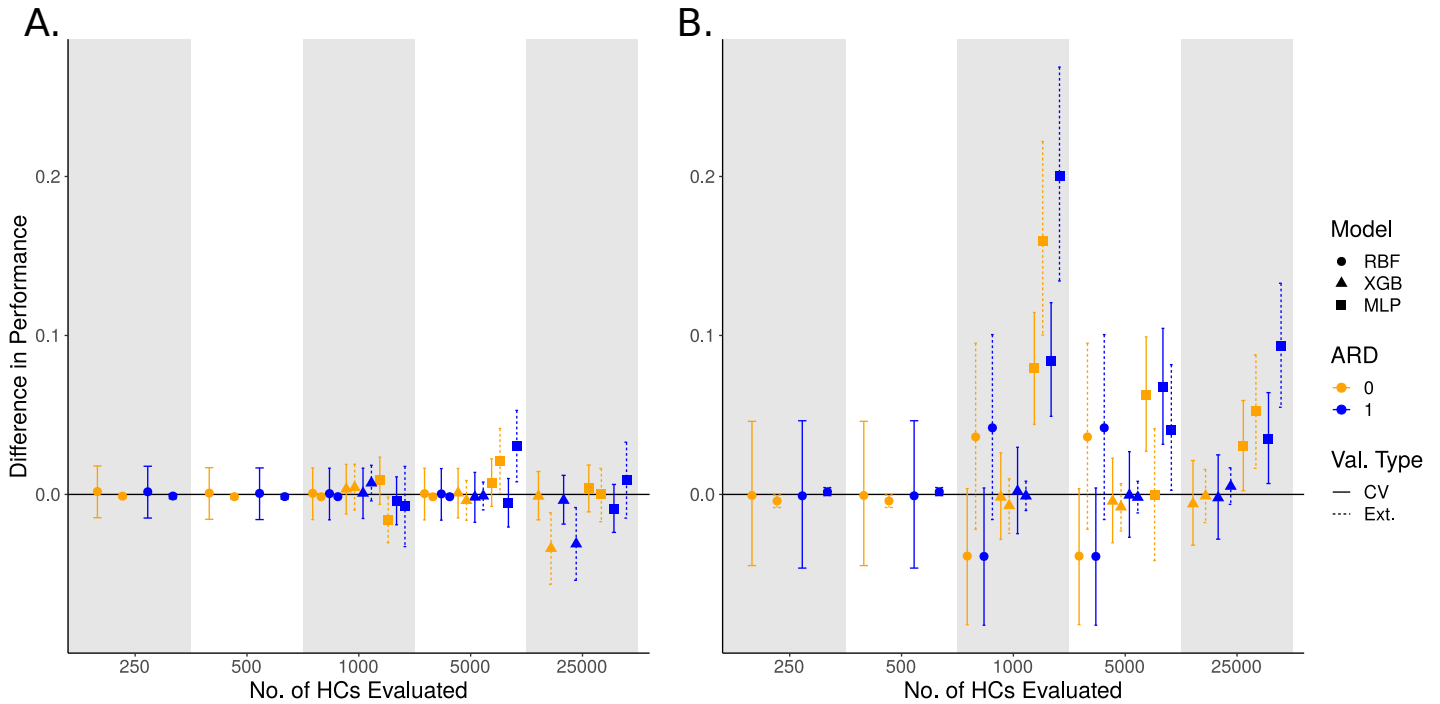


Figure 2: Differences in classifier performance in internal (CV) and external validation on the BVN (A; mAUC) and mortality (B; AUC) tasks for GS/RS evaluation budgets with the EI acquisition function and 5 initialization configurations in the *original* hyperparameter space. Similar layout to Figure 1 except that the indicated evaluation budgets only apply to GS/RS-selected classifiers. BO-selected classifiers are taken from 100-evaluation (RBF) or 500-evaluation (XGB and MLP) runs.

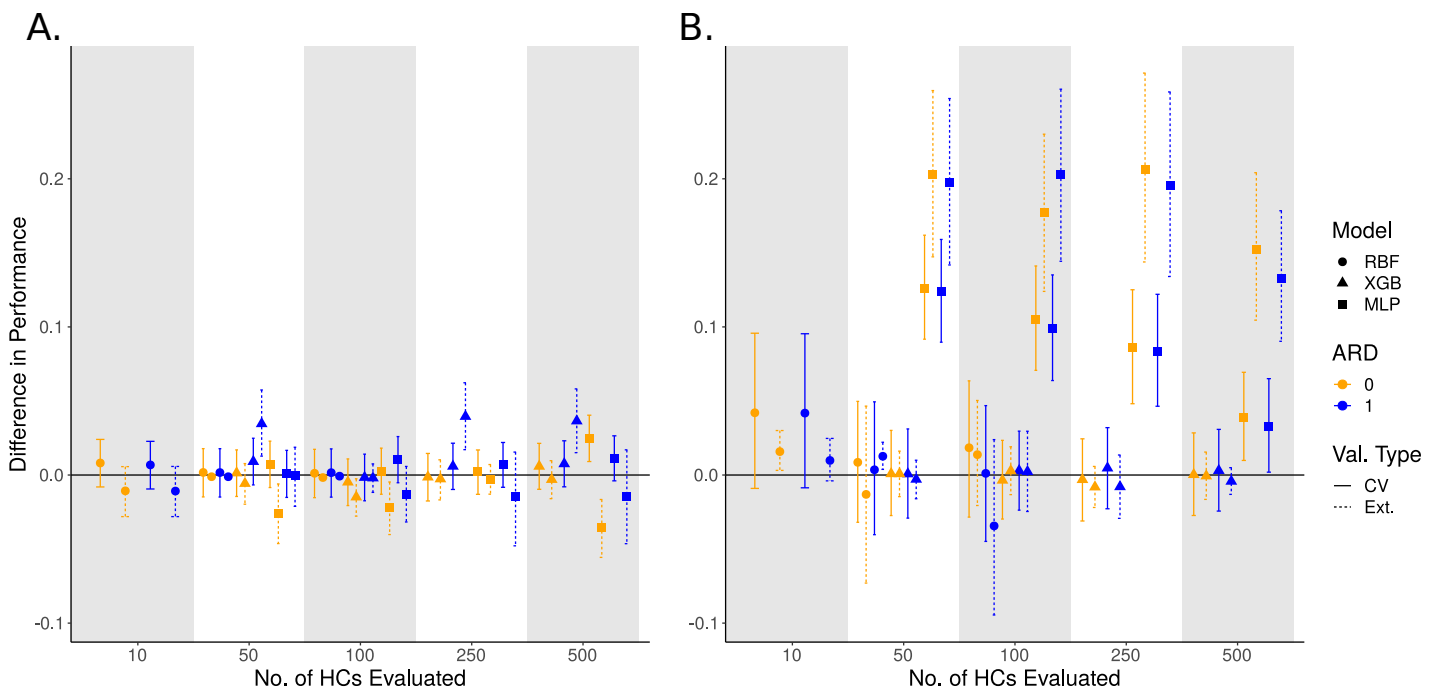


Figure 3: Differences in classifier performance in internal (CV) and external validation on the BVN (A; mAUC) and mortality (B; AUC) tasks for BO evaluation budgets with the UCB acquisition function and 25 initialization configurations in the *original* hyperparameter space. Differences greater than 0 indicate better performance for the BO-selected classifier. Classifiers were selected using either BO or GS/RS with the indicated number of evaluations. Points represent observed differences while error bars represent 95% bootstrap confidence intervals of the difference in performance.

Table 3: Grouped 5-fold CV and external validation (Val.) performance of selected classifiers for the BVN and mortality (Mort.) tasks. BO runs were performed in the *original* hyperparameter space with the EI acquisition function and 5 initialization configurations at the indicated evaluation budgets. **Bold** numbers indicate the best performance for a column.

Model	HO Type	No. of Evals.	ARD	BVN CV	BVN Val.	Mort. CV	Mort. Val.
RBF	GS	10	-	0.808	0.862	0.758	0.736
	GS	50	-	0.814	0.853	0.797	0.739
	GS	100	-	0.814	0.853	0.800	0.782
	GS	250	-	0.814	0.853	0.801	0.749
	GS	500	-	0.815	0.853	0.801	0.749
	GS	1000	-	0.815	0.853	0.839	0.708
	GS	5000*	-	0.815	0.853	0.839	0.708
	BO	10	Y	0.809	0.859	0.800	0.746
	BO	10	N	0.811	0.851	0.799	0.755
	BO	50	Y	0.816	0.851	0.800	0.749
	BO	50	N	0.815	0.852	0.800	0.745
	BO	100	Y	0.816	0.852	0.800	0.750
	BO	100	N	0.816	0.852	0.801	0.745
	XGB	RS	50	-	0.809	0.830	0.880
RS		100	-	0.813	0.827	0.885	0.819
RS		250	-	0.812	0.826	0.885	0.829
RS		500	-	0.810	0.829	0.885	0.826
RS		1000	-	0.810	0.822	0.885	0.822
RS		5000	-	0.813	0.830	0.888	0.823
RS		25000	-	0.815	0.860	0.889	0.816
BO		50	Y	0.809	0.822	0.883	0.819
BO		50	N	0.809	0.816	0.877	0.801
BO		100	Y	0.818	0.864	0.883	0.827
BO		100	N	0.812	0.827	0.889	0.827
BO		250	Y	0.812	0.834	0.888	0.827
BO		250	N	0.810	0.827	0.881	0.814
BO		500	Y	0.811	0.829	0.887	0.821
BO	500	N	0.814	0.826	0.883	0.815	
MLP	RS	50	-	0.818	0.860	0.762	0.631
	RS	100	-	0.814	0.863	0.785	0.640
	RS	250	-	0.824	0.861	0.807	0.625
	RS	500	-	0.819	0.859	0.853	0.691
	RS	1000	-	0.835	0.872	0.809	0.637
	RS	5000	-	0.837	0.835	0.826	0.796
	RS	25000	-	0.840	0.856	0.859	0.743
	BO	50	Y	0.822	0.847	0.888	0.833
	BO	50	N	0.817	0.864	0.883	0.819
	BO	100	Y	0.829	0.853	0.889	0.809
	BO	100	N	0.828	0.856	0.890	0.829
	BO	250	Y	0.828	0.854	0.886	0.800
	BO	250	N	0.833	0.850	0.888	0.820
	BO	500	Y	0.831	0.865	0.893	0.837
BO	500	N	0.844	0.856	0.889	0.796	

Table 4: Grouped 5-fold CV and external validation (Val.) performance of selected classifiers for the BVN and mortality (Mort.) tasks. BO runs were performed in the *original* hyperparameter space with the UCB acquisition function and 25 initialization configurations at the indicated evaluation budgets. **Bold** numbers indicate the best performance for a column.

Model	HO Type	No. of Evals.	ARD	BVN CV	BVN Val.	Mort. CV	Mort. Val.
RBF	GS	10	-	0.808	0.862	0.758	0.736
	GS	50	-	0.814	0.853	0.797	0.739
	GS	100	-	0.814	0.853	0.800	0.782
	GS	250	-	0.814	0.853	0.801	0.749
	GS	500	-	0.815	0.853	0.801	0.749
	GS	1000	-	0.815	0.853	0.839	0.708
	GS	5000*	-	0.815	0.853	0.839	0.708
	BO	10	Y	0.814	0.851	0.800	0.746
	BO	10	N	0.816	0.851	0.800	0.752
	BO	50	Y	0.816	0.852	0.801	0.752
	BO	50	N	0.816	0.852	0.806	0.726
	BO	100	Y	0.816	0.852	0.801	0.748
	BO	100	N	0.815	0.851	0.818	0.796
	XGB	RS	50	-	0.809	0.830	0.880
RS		100	-	0.813	0.827	0.885	0.819
RS		250	-	0.812	0.826	0.885	0.829
RS		500	-	0.810	0.829	0.885	0.826
RS		1000	-	0.810	0.822	0.885	0.822
RS		5000	-	0.813	0.830	0.888	0.823
RS		25000	-	0.815	0.860	0.889	0.816
BO		50	Y	0.818	0.865	0.881	0.816
BO		50	N	0.810	0.825	0.881	0.819
BO		100	Y	0.811	0.825	0.888	0.821
BO		100	N	0.808	0.812	0.882	0.822
BO		250	Y	0.818	0.865	0.890	0.821
BO		250	N	0.811	0.823	0.882	0.821
BO		500	Y	0.818	0.865	0.888	0.821
BO	500	N	0.816	0.826	0.885	0.825	
MLP	RS	50	-	0.818	0.860	0.762	0.631
	RS	100	-	0.814	0.863	0.785	0.640
	RS	250	-	0.824	0.861	0.807	0.625
	RS	500	-	0.819	0.859	0.853	0.691
	RS	1000	-	0.835	0.872	0.809	0.637
	RS	5000	-	0.837	0.835	0.826	0.796
	RS	25000	-	0.840	0.856	0.859	0.743
	BO	50	Y	0.820	0.860	0.886	0.828
	BO	50	N	0.826	0.834	0.889	0.833
	BO	100	Y	0.825	0.850	0.884	0.843
	BO	100	N	0.817	0.841	0.890	0.817
	BO	250	Y	0.831	0.846	0.891	0.820
	BO	250	N	0.826	0.858	0.893	0.831
	BO	500	Y	0.830	0.845	0.886	0.824
BO	500	N	0.844	0.824	0.892	0.844	

Table 5: Grouped 5-fold CV and external validation (Val.) performance of selected classifiers for the BVN and mortality (Mort.) tasks. BO runs were performed in the *transformed* hyperparameter space with the EI acquisition function and 25 initialization configurations at the indicated evaluation budgets. **Bold** numbers indicate the best performance for a column.

Model	HO Type	No. of Evals.	ARD	BVN CV	BVN Val.	Mort. CV	Mort. Val.
RBF	GS	10	-	0.808	0.862	0.758	0.736
	GS	50	-	0.814	0.853	0.797	0.739
	GS	100	-	0.814	0.853	0.800	0.782
	GS	250	-	0.814	0.853	0.801	0.749
	GS	500	-	0.815	0.853	0.801	0.749
	GS	1000	-	0.815	0.853	0.839	0.708
	GS	5000*	-	0.815	0.853	0.839	0.708
	BO	10	Y	0.813	0.851	0.817	0.678
	BO	10	N	0.815	0.852	0.832	0.772
	BO	50	Y	0.815	0.851	0.800	0.748
	BO	50	N	0.816	0.852	0.802	0.735
	BO	100	Y	0.816	0.852	0.810	0.727
	BO	100	N	0.816	0.852	0.801	0.749
	XGB	RS	50	-	0.809	0.830	0.880
RS		100	-	0.813	0.827	0.885	0.819
RS		250	-	0.812	0.826	0.885	0.829
RS		500	-	0.810	0.829	0.885	0.826
RS		1000	-	0.810	0.822	0.885	0.822
RS		5000	-	0.813	0.830	0.888	0.823
RS		25000	-	0.815	0.860	0.889	0.816
BO		50	Y	0.809	0.828	0.883	0.824
BO		50	N	0.811	0.827	0.882	0.815
BO		100	Y	0.810	0.826	0.885	0.824
BO		100	N	0.811	0.830	0.883	0.826
BO		250	Y	0.810	0.820	0.887	0.816
BO		250	N	0.811	0.817	0.886	0.823
BO		500	Y	0.814	0.823	0.889	0.823
BO	500	N	0.808	0.826	0.883	0.811	
MLP	RS	50	-	0.818	0.860	0.762	0.631
	RS	100	-	0.814	0.863	0.785	0.640
	RS	250	-	0.824	0.861	0.807	0.625
	RS	500	-	0.819	0.859	0.853	0.691
	RS	1000	-	0.835	0.872	0.809	0.637
	RS	5000	-	0.837	0.835	0.826	0.796
	RS	25000	-	0.840	0.856	0.859	0.743
	BO	50	Y	0.815	0.840	0.890	0.821
	BO	50	N	0.819	0.873	0.888	0.824
	BO	100	Y	0.822	0.878	0.893	0.836
	BO	100	N	0.817	0.858	0.889	0.837
	BO	250	Y	0.824	0.863	0.889	0.831
	BO	250	N	0.831	0.856	0.892	0.836
	BO	500	Y	0.833	0.858	0.890	0.833
BO	500	N	0.832	0.843	0.892	0.809	

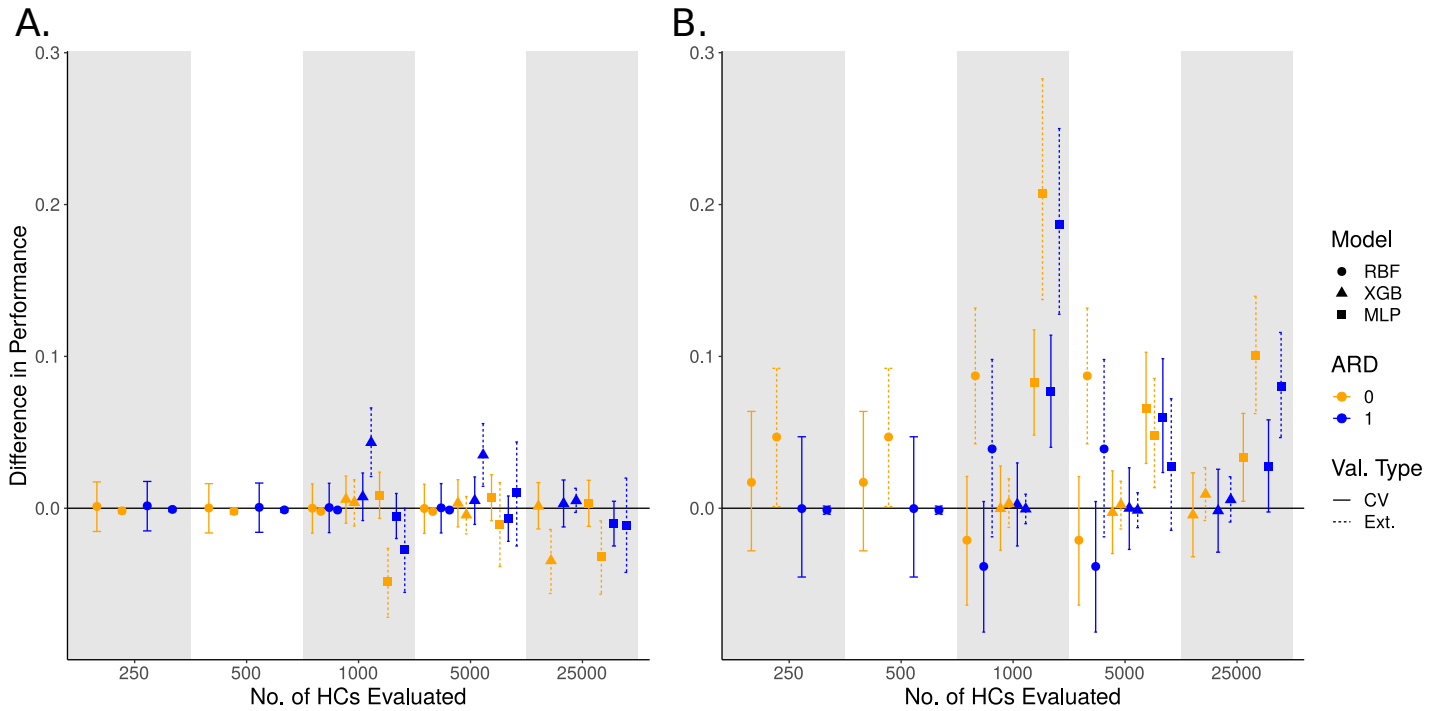


Figure 4: Differences in classifier performance in internal (CV) and external validation on the BVN (A; mAUC) and mortality (B; AUC) tasks for GS/RS evaluation budgets with the UCB acquisition function and 25 initialization configurations in the *original* hyperparameter space. Similar layout to Figure 3 except that the indicated evaluation budgets only apply to GS/RS-selected classifiers. BO-selected classifiers are taken from 100-evaluation (RBF) or 500-evaluation (XGB and MLP) runs.

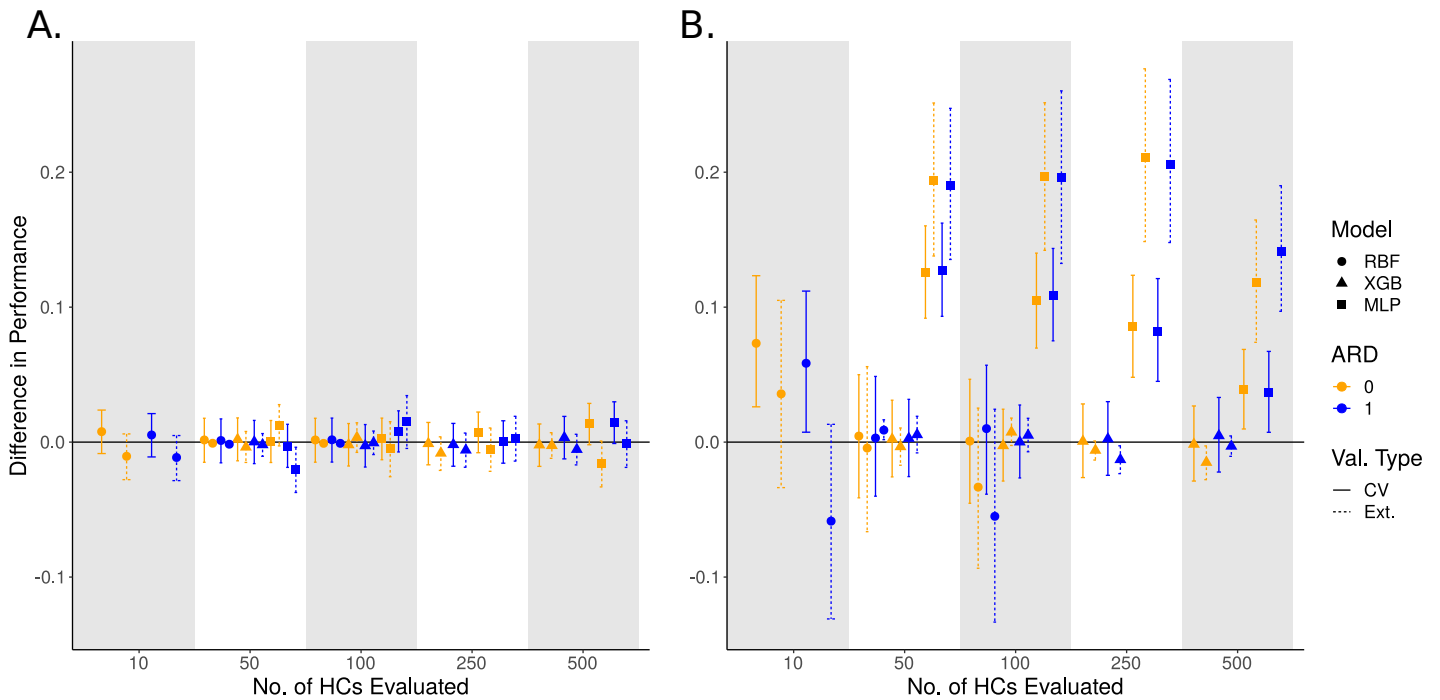


Figure 5: Differences in classifier performance in internal (CV) and external validation on the BVN (A; mAUC) and mortality (B; AUC) tasks for BO evaluation budgets with the EI acquisition function and 25 initialization configurations in the *transformed* hyperparameter space. Differences greater than 0 indicate better performance for the BO-selected classifier. Classifiers were selected using either BO or GS/RS with the indicated number of evaluations. Points represent observed differences while error bars represent 95% bootstrap confidence intervals of the difference in performance.

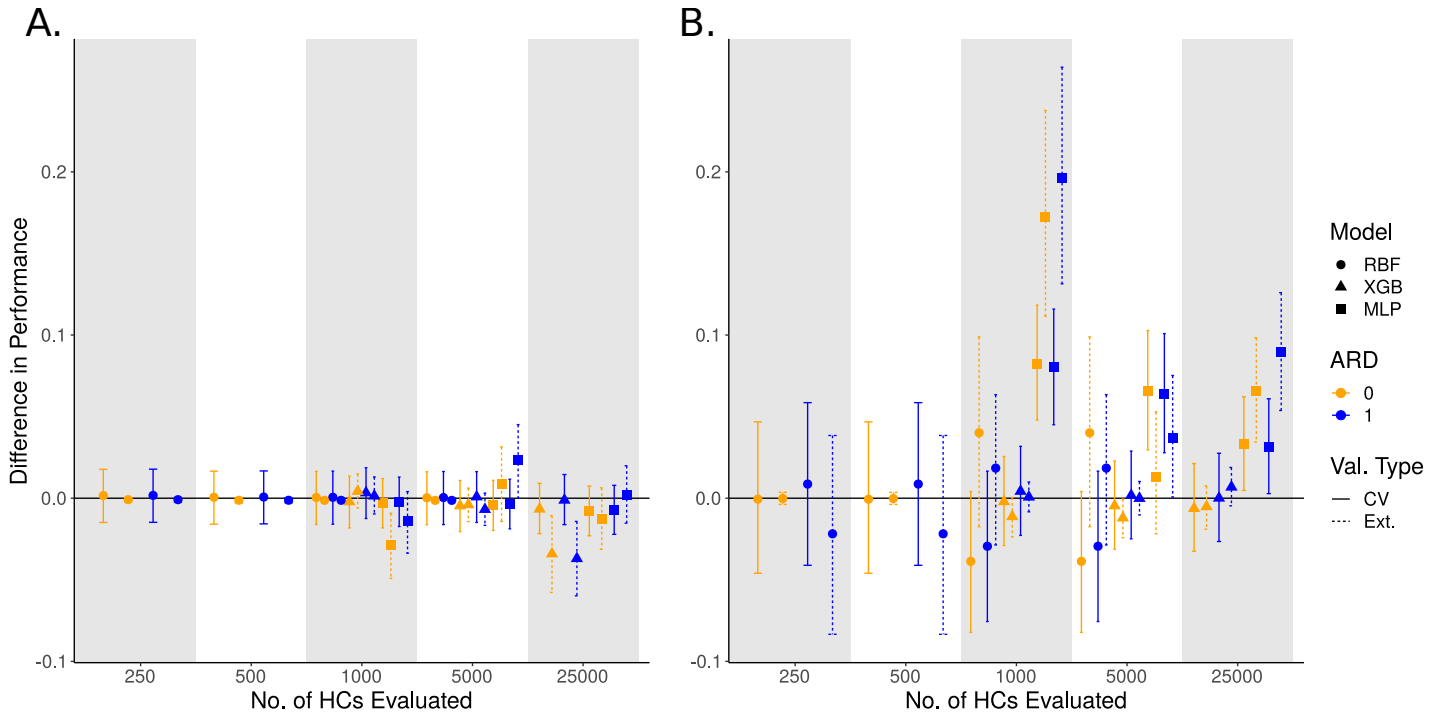


Figure 6: Differences in classifier performance in internal (CV) and external validation on the BVN (A; mAUC) and mortality (B; AUC) tasks for GS/RS evaluation budgets with the EI acquisition function and 25 initialization configurations in the *transformed* hyperparameter space. Similar layout to Figure 5 except that the indicated evaluation budgets only apply to GS/RS-selected classifiers. BO-selected classifiers are taken from 100-evaluation (RBF) or 500-evaluation (XGB and MLP) runs.

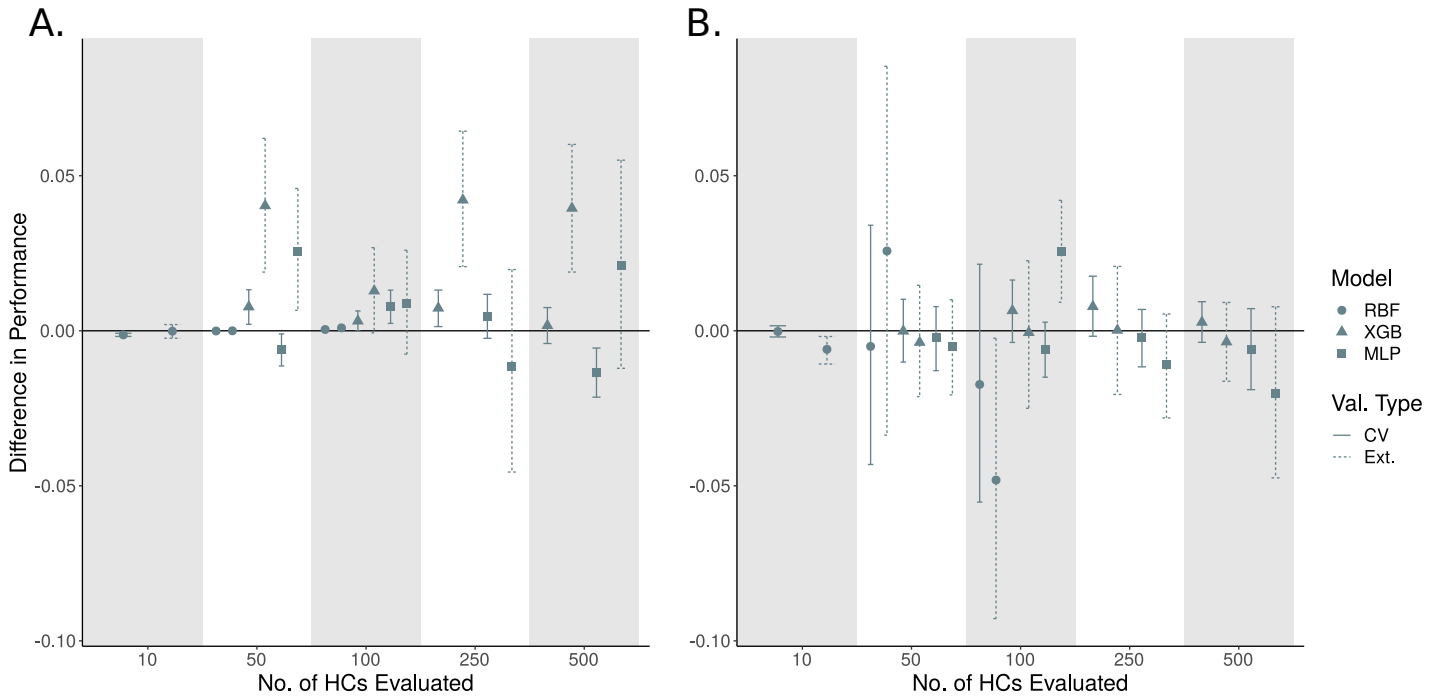


Figure 7: Differences in classifier performance in internal (CV) and external validation on the BVN (A; mAUC) and mortality (B; AUC) tasks for BO-selected classifiers with or without ARD enabled. BO runs were performed with the UCB acquisition function and 25 initialization configurations in the *original* hyperparameter space. Differences greater than 0 indicate better performance for the ARD-enabled classifier. Points represent observed differences while error bars represent 95% bootstrap confidence intervals of the difference in performance.

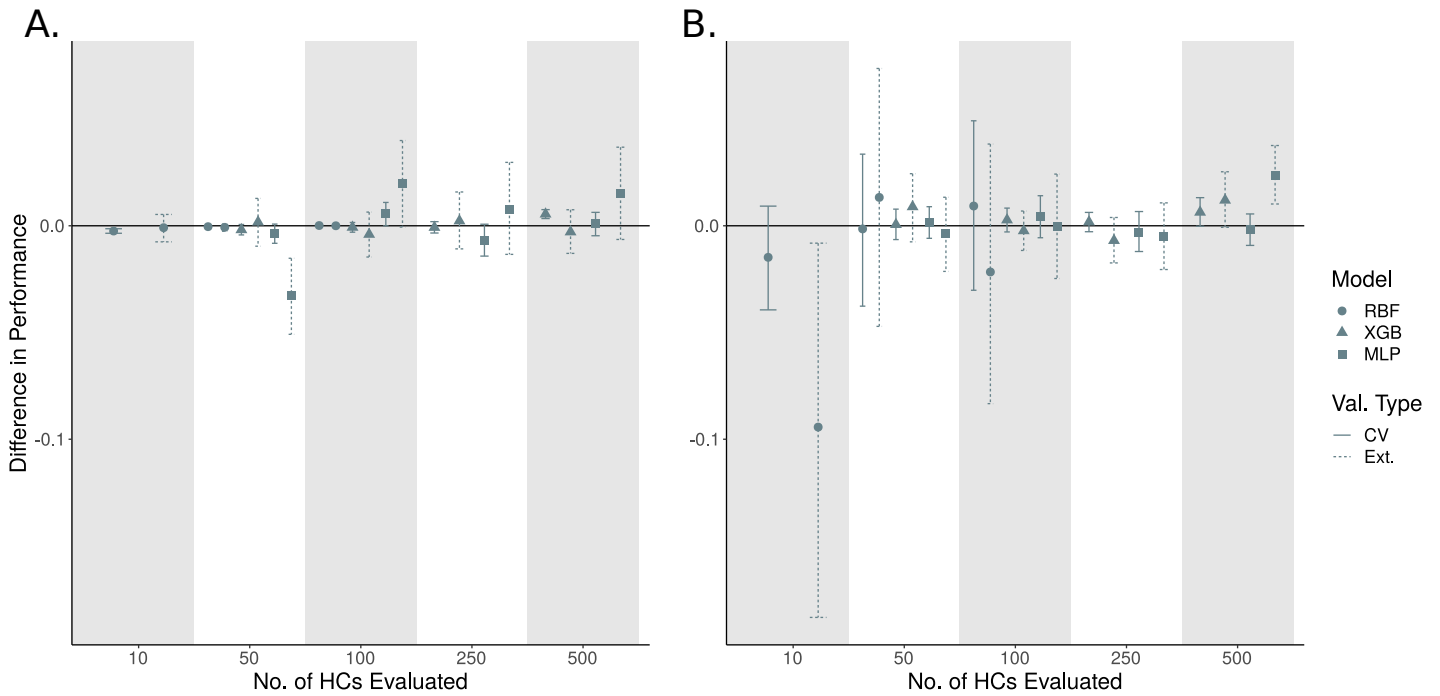


Figure 8: Differences in classifier performance in internal (CV) and external validation on the BVN (A; mAUC) and mortality (B; AUC) tasks for BO-selected classifiers with or without ARD enabled. BO runs were performed with the EI acquisition function and 25 initialization configurations in the *transformed* hyperparameter space. Differences greater than 0 indicate better performance for the ARD-enabled classifier. Points represent observed differences while error bars represent 95% bootstrap confidence intervals of the difference in performance.

References

- [1] Michael B. Mayhew, Ljubomir Buturovic, Roland Luethy, Uros Midic, Andrew R. Moore, Jonasel A. Roque, Brian D. Shaller, Tola Asuni, David Rawling, Melissa Rimmel, Kirindi Choi, James Wacker, Purvesh Khatri, Angela J. Rogers, and Timothy E. Sweeney. A generalizable 29-mrna neural-network classifier for acute bacterial and viral infections. *Nature Communications*, 11(1):1177, 2020.
- [2] TE Sweeney, TM Perumal, and R et al. Henao. A community approach to mortality prediction in sepsis via gene expression analysis. *Nat Commun*, (1), 2018.
- [3] TE Sweeney, Aaditya Shidham, Hector R Wong, and Purvesh Khatri. A comprehensive time-course-based multicohort analysis of sepsis and sterile inflammation reveals a robust diagnostic gene set. *Science Translational Medicine*, 7(287), 2015.
- [4] TE Sweeney, Hector R Wong, and Purvesh Khatri. Robust classification of bacterial and viral infections via integrated host gene expression diagnostics. *Science Translational Medicine*, 8(346), 2016.
- [5] The GPyOpt authors. GPyOpt: A Bayesian Optimization framework in python. <http://github.com/SheffieldML/GPyOpt>, 2016.